International Journal For Recent Developments in Science & Technology
2581-4575
Crossref
A Peer Reviewed Research Journal

PERTURBATION APPROACH WITH TEMPERATURE DEPENDENT HEAT SOURCE, JOULE HEATING, AND RADIATION ABSORPTION DURING MHD BOUNDARY LAYER FLOW ON AN INCLINED HEATED POROUS PLATE

P. Satyanarayana Reddy
Assistant professor, Department of Mathematics BJR Government Degree College, Narayanaguda, Hyderabad

Abstract:
Novel research of this work is to explore heat and mass transfer properties on MHD boundary layer flow of a viscous, incompressible, free convective, chemically reactive, radiative and electrically conducting fluid on a moving inclined heated porous plate in the presence of radiation absorption, temperature dependent heat source and joule heating is analyzed. The non-linear coupled partial differential equations are solved by perturbation technique. The impact of different pertinent parameters on velocity, temperature and concentration distribution have been studied and explored with the help of graphs. Further, the results of the skin friction coefficient and dimensionless rate of heat and mass transfer at the plate are also presented.
Keywords: boundary layer flow; free convective; moving inclined heated porous plate.

1. INTRODUCTION:

In many scientific and technological domains, such as the chemical industry and nuclear reactor cooling, convective heat and mass transfer fluxes over inclined porous plates play an important role. MHD power generators, petroleum engineering, methods for extracting geothermal energy, etc. These days, a lot of people are interested in studying convective heat and mass transfer flows with different physical features for flat plates that are either horizontal or vertical. There has been less focus on the boundary layer flows that are near to inclined plates or wedges, however. In the aforementioned research, the combined heat and mass transport issue in MHD free convection was examined, together with the impact of ohmic heating and viscous dissipation. Nevertheless, these two factors should be included for a more realistic investigation of the magnetic field's influence on boundary layer heat transport. Many processes rely on combined heat and mass transfer during chemical reactions, which is why this area of study has garnered a lot of interest recently. Heat and mass transfer happen concurrently in processes including drying, surface evaporation of water, energy transfer in a wet cooling tower, and movement in a desert cooler. Many different types of industries might potentially benefit from this flow. In the power sector, for instance, one way to generate electricity is to directly tap into the potential energy of a flowing conducting fluid.

There are several industrial uses for transport phenomena over inclined surfaces, including fuel combustion, condensation systems, magnetic thin film deposition, geothermal heat transmission from oblique faults, thermal coating, and geophysical debris flows. Since the thermal buoyancy force is directly proportional to the inclination angle, it is easy to adjust it

using an inclined plane in materials processing equipment. Non-Newtonian fluids are also present in materials production processes, such as plastic coating dynamics [7], gel and thin film systems [8], and ferrofluids based on Fe3O4 and kerosene or water [9]. The momentum and heat transmission properties of these flows are greatly affected by the rheology of the fluids involved. When working with thermoplastic sheets, the fluid elasticity, which is modulated by the Weissenberg number, may cause viscoelastic film flows to become unstable [10]. Subsequently, several rheological models have been used to investigate momentum and thermal boundary layer flows from slanted surfaces in the last few years. To account for the nonlinearity of these flows, these investigations have also made extensive use of sophisticated computational approaches. In their study, Nsom et al. [11] examined the stability of shear-thinning fluid past an inclined plane with coating process and natural hazards using the power-law fluid model and perturbation approach. According to their findings, the relative fluctuation of the crucial Reynolds number grows as the wave number rises and shrinks when the power-law index increases. Using a perturbation approach, Anandamony and Souradip [12] analyzed the instability of a thin liquid film flowing across an inclined plane, taking into account fluctuations in density, dynamic viscosity, surface tension, and thermal diffusivity. The hydromagnetic and radiation effects on solid-gas flows via an inclined plane were investigated by Mehmood et al. [13] using the bvp4c package. Both the gas-particle interaction and the Grashof number were shown to have an effect on the velocity profile of the gas and dust phases.

Combustible boundary layer flows over a hot inclined surface were studied by Roy et al. [14] in relation to fluctuations in sinusoidal surface temperature. As the angle of inclination increased, they noticed a notable rise in the heat and mass transmission boundary layer. In their presentation, Sulochana et al. [15] demonstrated the maximum shear flow (MHD) of Casson nanofluid via a chemical reaction-perturbing semi-infinitely angled porous plate. Heat and mass transfer speeds are both accelerated by the radiation and chemical reaction factors, as they noticed. Researchers Sui et al. [16] examined mixed convection flows from a moving conveyor over an inclined plate using the power-law fluid and homotopy analysis approach. When the inclination angle was reduced, they found that the flow decreased, but the thermal boundary layer flow increased. Natural convection over heated inclined surfaces of varied inclinations (from horizontal to vertical) was studied in the computational fluid dynamics (CFD) work by Abhijit et al. [17]. At the lift-of point, when the natural convective boundary layer becomes a free plume, they spoke about its quantitative and qualitative behavior. Both power-law and micropolar fluid flows have been the subject of very few recent investigations [18, 19, 20].

Motivated by the above studies, in this chapter heat and mass transfer properties on MHD boundary layer flow of a viscous, incompressible, free convective, chemically reactive, radiative and electrically conducting fluid on a moving inclined heated porous plate in the presence of radiation absorption, temperature dependent heat source and joule heating is analyzed. The non-linear coupled partial differential equations are solved by perturbation

International Journal For Recent Developments in Science & Technology
2581-4575
Crossref
A Peer Reviewed Research Journal

technique. The impact of different pertinent parameters on velocity, temperature and concentration distribution have been studied and explored with the help of graphs. Further, the results of the skin friction coefficient and dimensionless rate of heat and mass transfer at the plate are also presented.

2. MATHEMATICAL FORMULATION:

Here a free convective laminar boundary layer flow of a viscous, incompressible, electrically conducting, chemically reactive, radiative, and heat-absorbing fluid past a semi-infinite moving permeable plate embedded in a uniform porous medium inclined at an angle ϕ is assumed. The fluid is subject to thermal and concentration buoyancy effects, as well as Joule's dissipation and a heat source that depends on temperature.

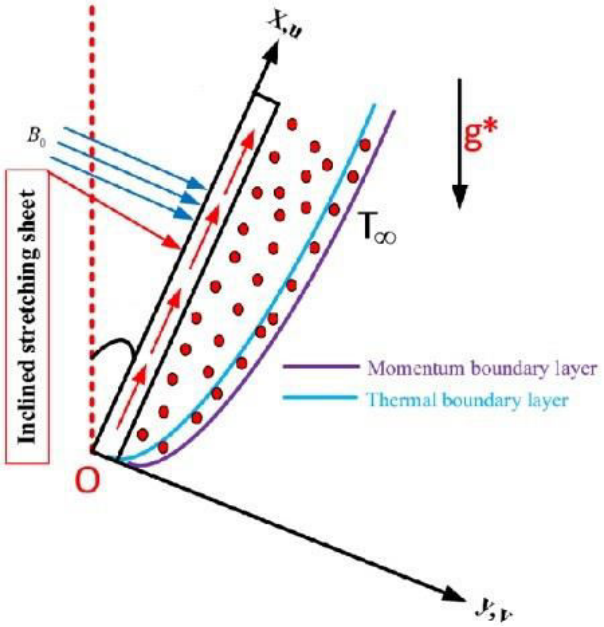

Fig.1: Geometry of the flow problem

Based on our findings, we hypothesised

1. The induced magnetic field may be disregarded due to the tiny Eckert number Ec.
2. A temperature (Tw) and concentration (Cw) greater than the ambient temperature (T∞) and concentration (C∞) correspondingly are maintained on the wall.
3. The diffusing species and the fluid are involved in a first-order homogeneous chemical process that has a rate constant.

In light of these physical factors, the following are the equations that control the fluid in a Cartesian coordinate system:

$$\frac{\partial v}{\partial y} = 0 \quad \Rightarrow \quad v^* = -V_0 \qquad (1)$$

Momentum Equation

International Journal For Recent Developments in Science & Technology
2581-4575
Crossref
A Peer Reviewed Research Journal

$$\rho v^* \frac{\partial u^*}{\partial y^*} = \mu \frac{\partial^2 u^*}{\partial y^{*2}} - \frac{\mu}{K} u^* - \sigma B_0^2 u^* + \rho g \cos\phi \beta_T (T^* - T_\infty) + \rho g \cos\phi \beta_C (C^* - C_\infty) \quad (2)$$

Energy Equation

$$\rho C_p v^* \frac{\partial T^*}{\partial y^*} = \alpha_1 \frac{\partial^2 T^*}{\partial y^{*2}} + \mu \left(\frac{\partial u^*}{\partial y^*} \right)^2 - \frac{\partial q_r^*}{\partial y^*} + \sigma B_0^2 u^{*2} - Q_0 \frac{\partial}{\partial y^*} (T^* - T_\infty) + R_A (C^* - C_\infty) \quad (3)$$

Concentration Equation

$$v^* \frac{\partial C^*}{\partial y^*} = D \frac{\partial^2 C^*}{\partial y^{*2}} - R(C^* - C_\infty) \quad (4)$$

The radiative heat flux $\frac{\partial q_r^*}{\partial y^*} = 4(T^* - T_\infty) I'$ (5)

Where $I' = \int_0^\infty K_{\lambda w} \frac{\partial e_{b\lambda}}{\partial T^*} d\lambda$, $K_{\lambda w}$ is the absorption coefficient at the wall and $e_{b\lambda}$ is Plank's function.

The proper boundary conditions for the fields of concentration, temperature, and velocity are specified as

$$u^* = u_p^*, \quad T^* = T_w, \quad C^* = C_w \qquad at \quad y = 0 \quad (6)$$

$$u^* \to 0, \quad T^* \to T_\infty, \quad C^* \to C_\infty \qquad as \quad y \to \infty \quad (7)$$

Introducing the following non-dimensional quantities

$$u = \frac{u^*}{v_0}, \upsilon = \frac{\mu}{\rho}, R_1 = \frac{\upsilon (C_w - C_\infty) R_A}{v_0^2 \rho C_p (T_w - T_\infty)}, y = \frac{v_0 y^*}{\upsilon}, u_p = \frac{u_p^*}{v_0}, M^2 = \frac{B_0^2 \upsilon^2 \sigma}{v_0^2 \mu}, K = \frac{K^* v_0^2}{\upsilon^2},$$

$$\theta = \frac{T^* - T_\infty}{T_w - T_\infty}, C = \frac{C^* - C_\infty}{C_w - C_\infty}, Sc = \frac{\upsilon}{d}, \gamma = \frac{R\upsilon}{v_0^2}, \Pr = \frac{\mu Cp}{\alpha_1}, H = \frac{Q_0}{\rho C_p v_0^3}, F = \frac{4\upsilon I'}{\rho C_p v_0^2},$$

$$Ec = \frac{v_0^2}{C_p (T_w - T_\infty)}, Gr = \frac{\rho g \beta_T \upsilon^2 (T_w - T_\infty)}{v_0^3 \mu}, Gc = \frac{\rho g \beta_C \upsilon^2 (C_w - C_\infty)}{v_0^3 \mu} \quad (8)$$

The basic field equations (2) – (4), can be expressed in non-dimensional form as

$$\frac{\partial^2 u}{\partial y^2} + \frac{\partial u}{\partial y} - \left(M + \frac{1}{K} \right) u = -Gr\theta \cos\phi - GmC \cos\phi \quad (9)$$

$$\frac{\partial^2 \theta}{\partial y^2} + \Pr(1 - H) \frac{\partial \theta}{\partial y} + \Pr Ec \left(\frac{\partial u}{\partial y} \right)^2 + \Pr EcM^2 u^2 = \Pr F\theta - \Pr R_1 C \quad (10)$$

$$\frac{\partial^2 C}{\partial y^2} + Sc \frac{\partial C}{\partial y} - Sc \gamma C = 0 \quad (11)$$

The corresponding boundary conditions in non-dimensional form are:

International Journal For Recent Developments in Science & Technology
2581-4575
Crossref
A Peer Reviewed Research Journal

$$u = u_p, \quad \theta = 1, \quad C = 1 \quad at \quad y = 0 \tag{12}$$

$$u \to 0, \quad \theta \to 0, \quad C \to 0 \quad as \quad y \to \infty \tag{13}$$

3. SOLUTION OF THE PROBLEM:

The set of partial differential equations (9) – (11) cannot be solved in closed form. However, they can be solved analytically after reducing them into a set of ordinary differential equations by taking the expressions for velocity *u(y),* temperature *θ(y)* and concentration *C(y)* in dimensionless form as follows:

$$u(y) = u_0(y) + E_C u_1(y) + O(E_C^2) \tag{1}$$

$$\theta(y) = \theta_0(y) + E_C \theta_1(y) + O(E_C^2) \tag{2}$$

$$C(y) = C_0(y) + E_C C_1(y) + O(E_C^2) \tag{3}$$

Substituting (1) – (3) in (9) – (11) and equating the coefficients of zeroth order of Eckert number(constants), equating the coefficients of the first order of Eckert number, andneglecting the higher order of $O(E_c^2)$ and after simplifying we get the following set of equations

$$u_0'' + u_0' - pu_0 = -Gr\theta_0 \cos\phi - GmC_0 \cos\phi \tag{4}$$

$$\theta_0'' + \Pr(1-H)\theta_0' - \Pr F\theta_0 = -\Pr R_1 C_0 \tag{5}$$

$$C_0'' + ScC_0' - Sc\,\gamma\, C_0 = 0 \tag{6}$$

$$u_1'' + u_1' - pu_1 = -Gr\theta_1 \cos\phi - GmC_1 \cos\phi \tag{7}$$

$$\theta_1'' + pr(1-H)\theta_1' - \Pr F\theta_1 = -\Pr u_0'^2 - \Pr M^2 u_0^2 - \Pr R_1 C_1 \tag{8}$$

$$C_1'' + ScC_1' - Sc\,\gamma\, C_1 = 0 \tag{9}$$

Where prime denotes ordinary differentiation with respect to 'y' and $p = M^2 + \frac{1}{K}$

The corresponding boundary conditions are:

$$u_0 = u_p, u_1 = 0, \theta_0 = 1, \theta_1 = 0, C_0 = 1, C_1 = 0 \quad at \quad y = 0 \tag{10}$$

$$u_0 \to 0, u_1 \to 0, \theta_0 \to 0, \theta_1 \to 0, C_0 \to 0, C_1 \to 0 \quad as \quad y \to \infty \tag{11}$$

Using boundary conditions (10) and (11), the solutions of (4) – (9), we obtain the following expressions for velocity, temperature and concentration.

$$u_0 = z_5 e^{-m_3 y} - z_3 e^{-m_2 y} - z_4 e^{-m_1 y} \tag{12}$$

$$\theta_0 = z_1 e^{-m_1 y} + z_2 e^{-m_2 y} \tag{13}$$

$$C_0 = e^{-m_1 y} \tag{14}$$

International Journal For Recent Developments in Science & Technology
2581-4575
Crossref
A Peer Reviewed Research Journal

$$u_1 = z_{26}e^{-m_5 y} - z_{19}e^{-m_4 y} + z_{20}e^{-2m_3 y} + z_{21}e^{-2m_2 y} + z_{22}e^{-2m_1 y} - z_{23}e^{-m_6 y} + z_{24}e^{-m_7 y} - z_{25}e^{-m_8 y} \quad (15)$$

$$\theta_1 = z_{18}e^{-m_4 y} - z_{12}e^{-2m_3 y} - z_{13}e^{-2m_2 y} - z_{14}e^{-2m_1 y} + z_{15}e^{-m_6 y} - z_{16}e^{-m_7 y} + z_{17}e^{-m_8 y} \quad (16)$$

$$C_1 = 0 \quad (17)$$

Substituting the above solutions (12) – (17) in (1) – (3), we get the final form of Velocity, Temperature, Concentration distributions in the boundary layer as follows

$$u(y) = \left[Z_5 e^{-m_3 y} - Z_3 e^{-m_2 y} - Z_4 e^{-m_1 y}\right] + Ec\left[\begin{array}{l} z_{26}e^{-m_5 y} - z_{19}e^{-m_4 y} + z_{20}e^{-2m_3 y} + z_{21}e^{-2m_2 y} + z_{22}e^{-2m_1 y} - z_{23}e^{-m_6 y} \\ + z_{24}e^{-m_7 y} - z_{25}e^{-m_8 y} \end{array}\right] \quad (18)$$

$$\theta(y) = \left[z_2 e^{-m_2 y} + z_1 e^{-m_1 y}\right] + Ec\left[\begin{array}{l} z_{18}e^{-m_4 y} - z_{12}e^{-2m_3 y} - z_{13}e^{-2m_2 y} - z_{14}e^{-2m_1 y} + z_{15}e^{-m_6 y} \\ - z_{16}e^{-m_7 y} + z_{17}e^{-m_8 y} \end{array}\right] \quad (19)$$

$$C(y) = e^{-m_1 y} \quad (20)$$

The physical quantities of interest are the wall shear stress τ_w is given by

$$\tau_w = \mu \left.\frac{\partial u^*}{\partial y^*}\right|_{y^*=0} = \rho v_0^2 u'(0)$$

The local skin friction factor τ is given by

$$\tau = \frac{\tau_w}{\rho v_0^2} = u'(0) = \left[-m_3 Z_5 + m_2 Z_3 + m_1 Z_4\right] + Ec\left[\begin{array}{l} -m_5 Z_{26} + m_4 Z_{19} - 2m_3 Z_{20} - 2m_2 Z_{21} \\ -2m_1 Z_{22} + m_6 Z_{23} - m_7 Z_{24} + m_8 Z_{25} \end{array}\right] \quad (21)$$

The local surface heat flux is given by: $q_w = -\kappa \left.\frac{\partial T^*}{\partial y^*}\right|_{y^*=0}$

The local Nusselt number $Nu_x = \frac{q_w}{(T_w - T_\infty)}$ can be written as

$$\frac{Nu_x}{\mathrm{Re}_x} = -\left.\frac{\partial \theta}{\partial y}\right|_{y=0} = \left[m_1 Z_1 + m_2 Z_2\right] - Ec\left[\begin{array}{l} -m_4 Z_{18} + 2m_3 Z_{12} + 2m_2 Z_{13} + 2m_1 Z_{14} \\ -m_6 Z_{15} + m_7 Z_{15} + m_7 Z_{16} - m_8 Z_{17} \end{array}\right] \quad (22)$$

The local surface mass flux is given by

International Journal For Recent Developments in Science & Technology
2581-4575
Crossref
A Peer Reviewed Research Journal

$$\frac{Sh_x}{\mathrm{Re}_x} = -\frac{\partial C}{\partial y}\bigg|_{y=0} = -m_1 \qquad (23)$$

Where $\mathrm{Re}_x = \frac{v_0 x}{\upsilon}$ is the local Reynolds number.

4. RESULTS AND DISCUSSION:

This research looks at how radiation absorption R1 and chemical reaction γ affect the flow of heat and mass during transient free convection in a moving inclined porous plate with a heat source that depends on temperature, as well as radiative flow and MHD free convective joule heating. Analytical studies have been conducted on the impacts of different factors on velocity, temperature, and concentration, and these effects have been shown using figures. The impact of the Hartmann number (M) is seen in Figure 2. The velocity profiles are shown to progressively shrink as the values of M rise. The peak value is where the influence of the magnetic field is most noticeable; as the field strength increases, the peak value falls sharply. This is due to the fact that electrically conducting fluids contain a force known as the Lorentz force, which acts counter to the flow when the field is applied in a normal direction, as it is in this problem. As can be seen in the illustration, this kind of resistance causes the fluid's velocity to decrease. For a variety of porosity parameter (K) values, the velocity profile is shown in Figure 3. Acceleration is proportional to the square of K. The influence of the angle of inclination () on the velocity profile is seen in Figure 4. We found that when the angle of inclination increases, the velocity drops. The influence of the thermal Grashof number (Gr) on the velocity profile is seen in Figure 5. The graphic clearly shows that when the thermal Grashof number grows, the velocity drops. Typical boundary layer velocity patterns for different values of the modified Grashof number are shown in Figure 6. As one moves closer to the plate surface, the velocity distribution reaches a peak and then gradually decreases until it approaches the free stream value. An increase in the concentration buoyancy effects, as expressed by a modified Grashof number, causes the fluid velocity to rise and makes the peak value more noticeable, as predicted. As the modified Grashof number grows, the value of velocity also increases, proving this point. Various values of the radiation parameter (F) are shown in Figure 7's velocity profiles. It is evident that the peak values of the velocity tend to grow as the radiation parameter increases. Figure 8 shows the velocity profiles for various values of the Schmidt number (Sc). A drop in boundary layer velocity is a natural consequence of a larger Schmidt number. Various values of Prandtlnumber are shown in Figure 9 by means of velocity profiles. When the Prandtl number is increased, the velocity is shown to decrease. Figure 10 shows how the velocity profile is affected by the radiation absorption parameter (R1). The fluid velocity is shown to decrease as the radiation absorption parameter increases. As shown in Figure 11, the velocity profiles vary for various values of the heat source parameter (H). The velocity distribution is more skewed as H gets higher.

Figure 12 shows how the temperature profile is affected by the radiation parameter (F). When the temperature drops, F goes up. Figure 13 displays temperature trends for various values of the radiation absorption parameter (R1). As the radiation absorption parameter is increased, the temperature of the fluid rises. The temperature profiles for various Prandtlnumber values

International Journal For Recent Developments in Science & Technology
2581-4575
Crossref
A Peer Reviewed Research Journal

are shown in Figure 14. It has been noted that when the Prandtl number increases, the temperature decreases. For larger values of the Prandtl number, heat may diffuse away from the heated surface more quickly since lower values of the number are comparable to increases in the fluid's thermal conductivity. Because of this, the thermal boundary layer is thicker and the heat transfer rate is lower when the Prandtl number is less. Figure 15 shows the temperature effect of the heat source parameter H. The graph clearly shows that as H grows, so does the temperature. Figure 16 shows the temperature profiles for various Schmidt numbers. As one may expect, the boundary layer temperature drops as the Schmidt number rises. For various values of the chemical reaction parameter γ, Figure 17 shows the behavior of concentration. It has been noted that as γ increases, concentration levels drop. Figure 18 shows how the concentration profiles change depending on the Schmidt number Sc. A lower concentration is seen with higher Schmidt numbers.

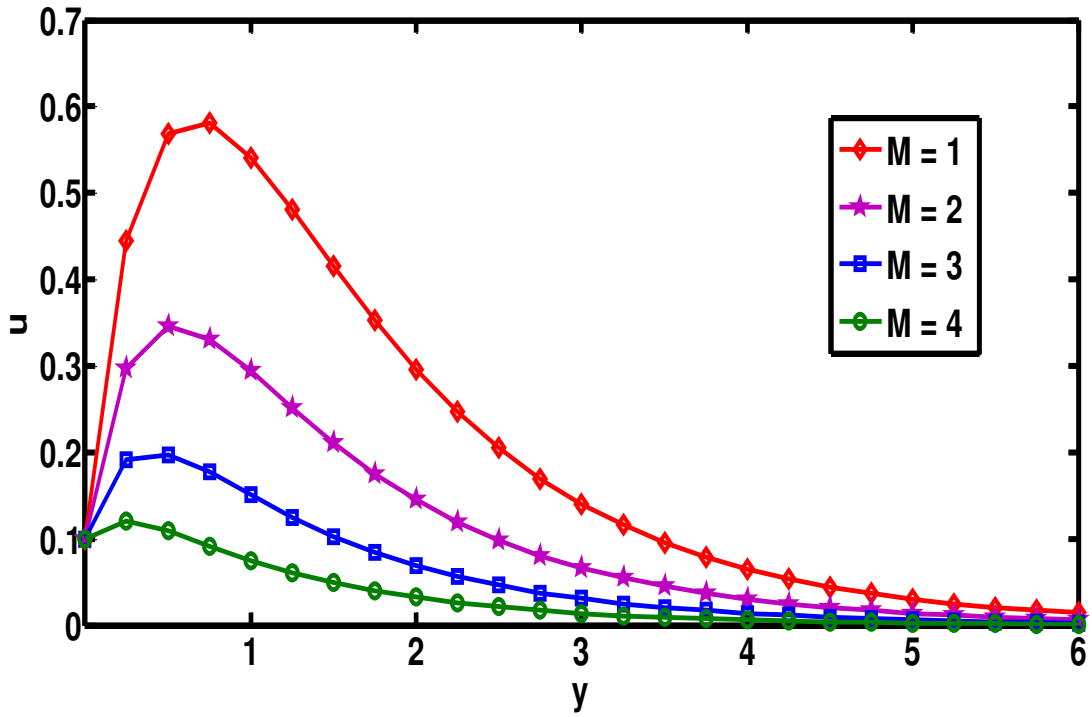

Figure 2: The u(y) profiles for Hartmann number M

International Journal For Recent Developments in Science & Technology
2581-4575
Crossref
A Peer Reviewed Research Journal

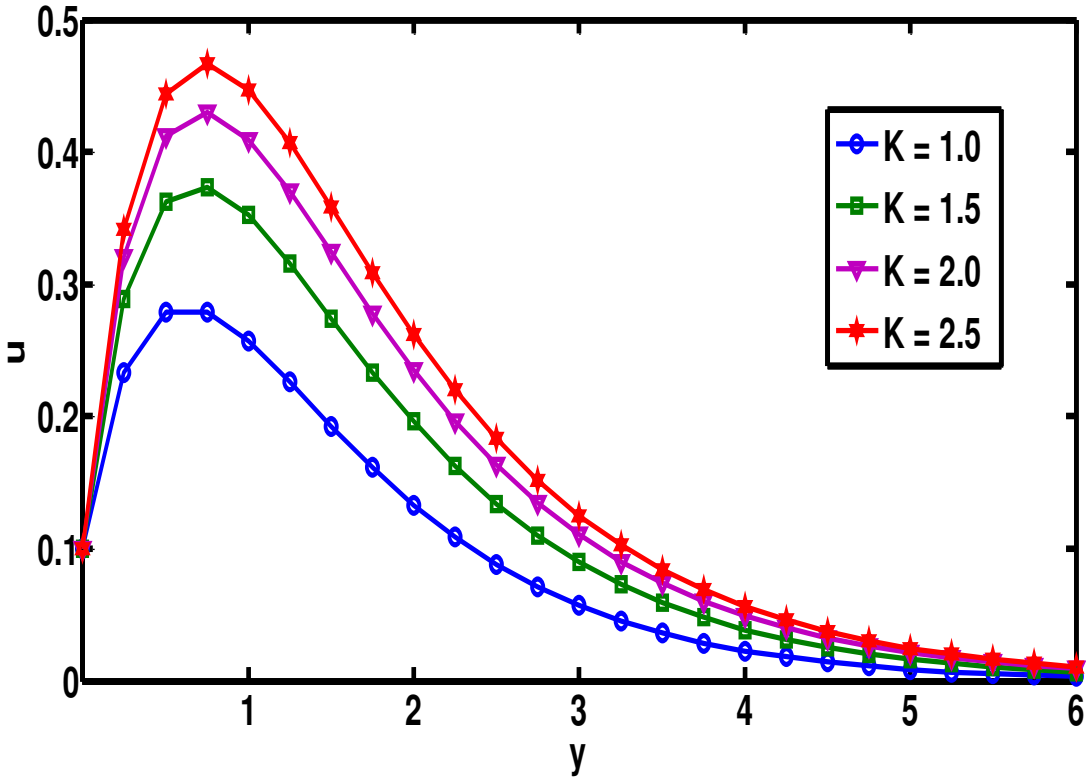

Figure 3: The u(y) profiles for porosity parameter K

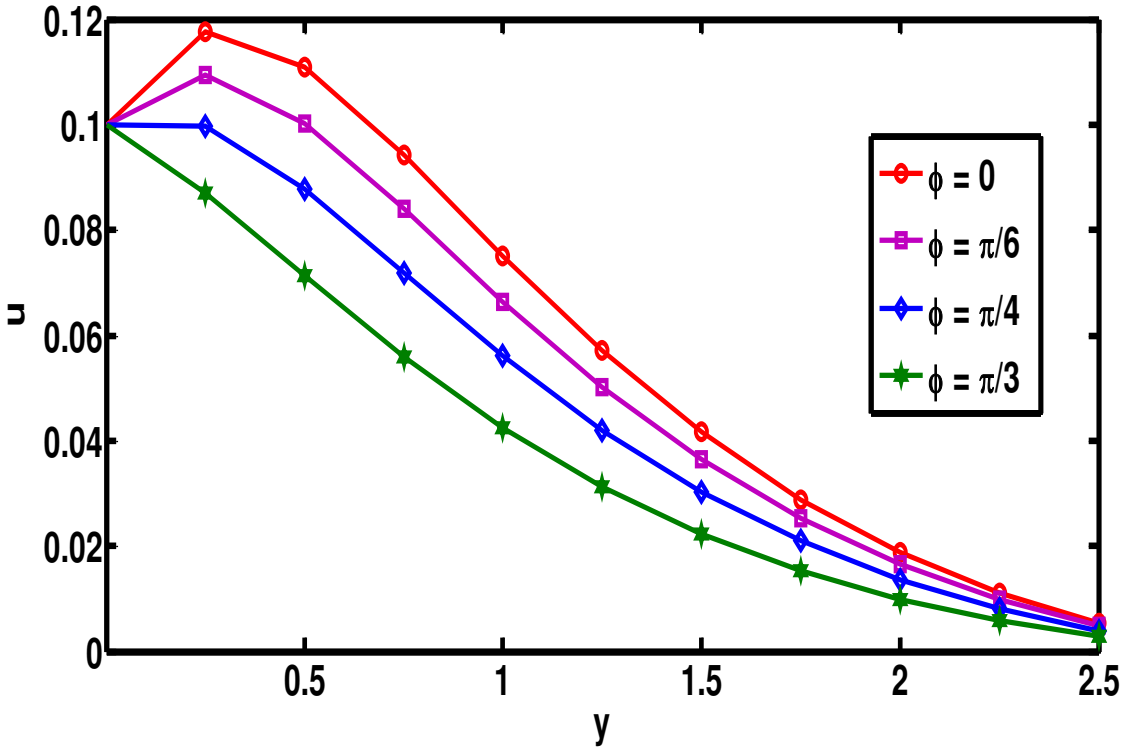

Figure 4: The u(y) profiles for angle of inclination ϕ

International Journal For Recent Developments in Science & Technology
2581-4575
Crossref
A Peer Reviewed Research Journal

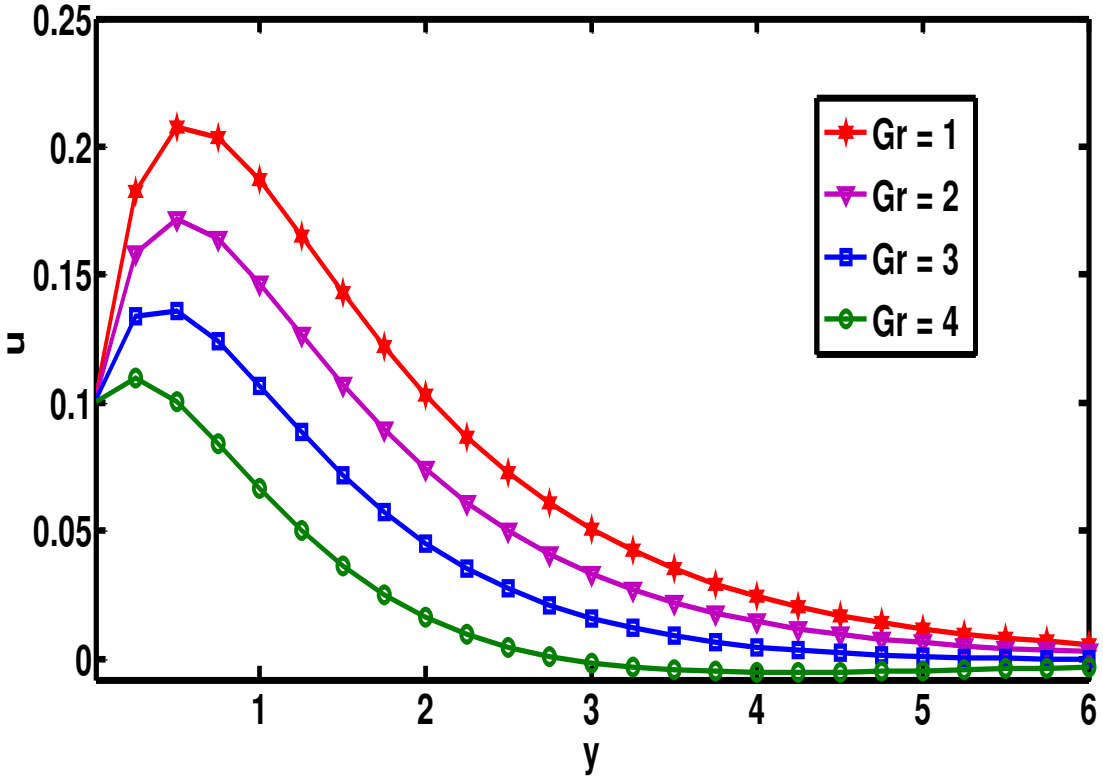

Figure 5: The u(y) profiles for Grashof number Gr

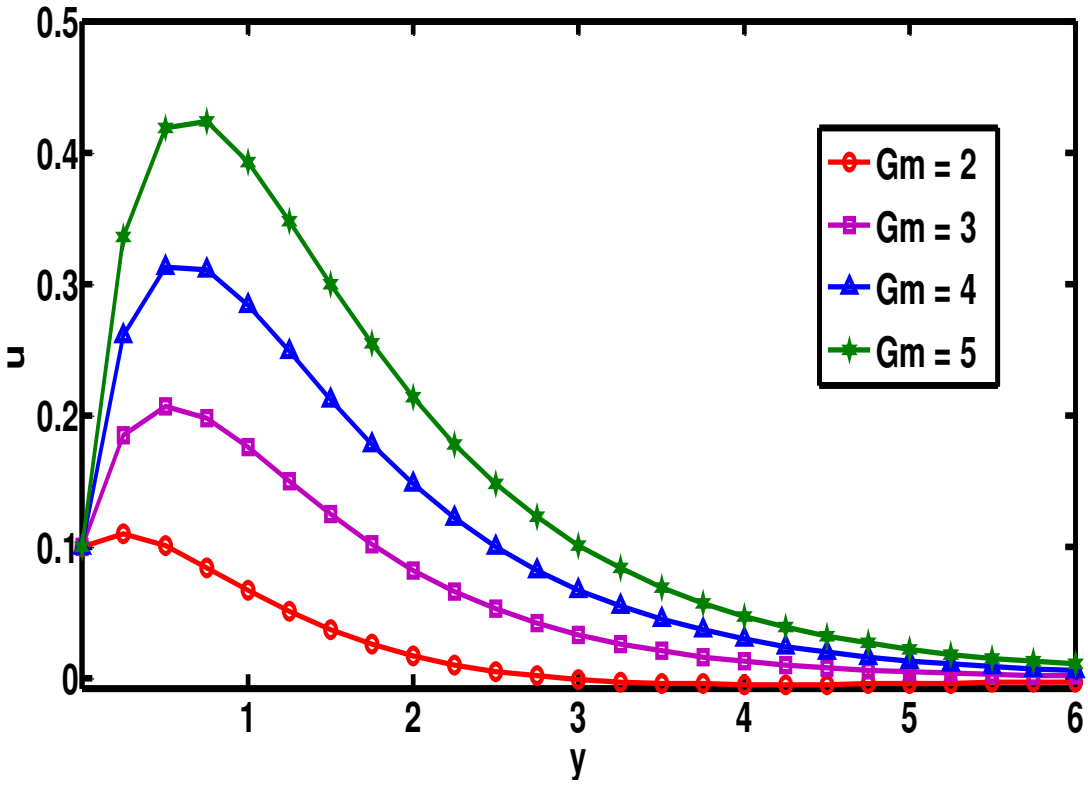

Figure 6: The u(y) profiles for of Gm

2581-4575
International Journal For Recent Developments in Science & Technology
Crossref
A Peer Reviewed Research Journal

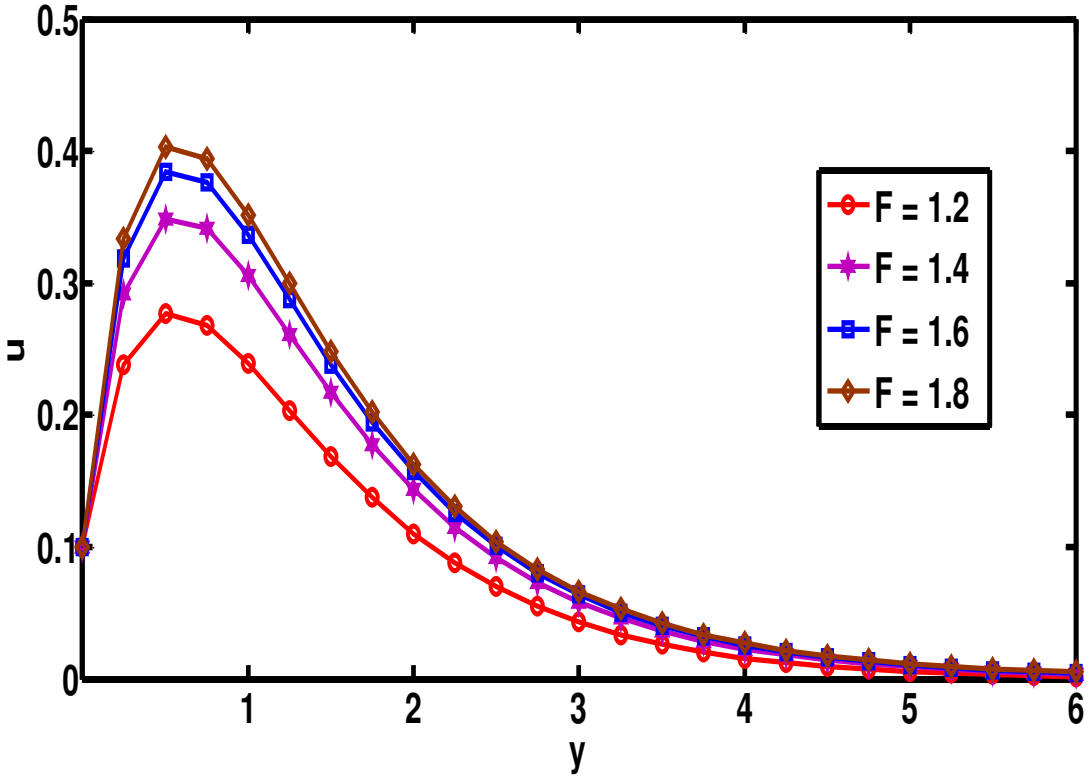

Figure 7: The u(y) profiles for radiation parameter F

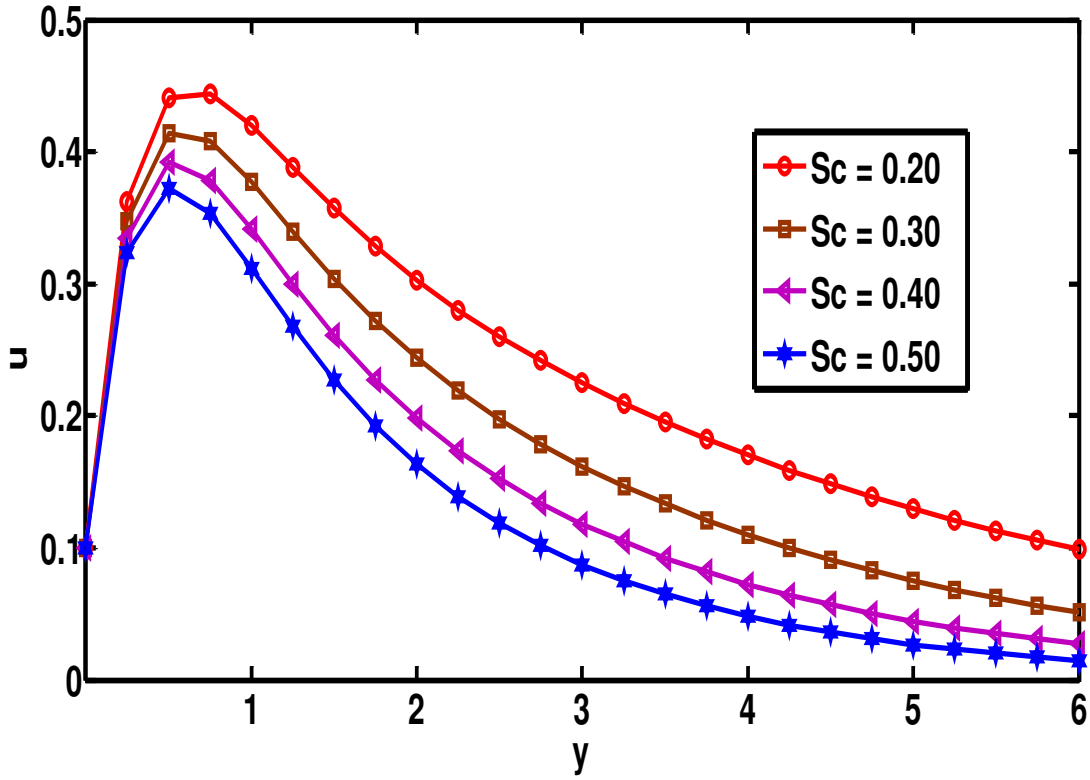

Figure 8: The u(y) profiles for Schmidt number Sc

International Journal For Recent Developments in Science & Technology
2581-4575
Crossref
A Peer Reviewed Research Journal

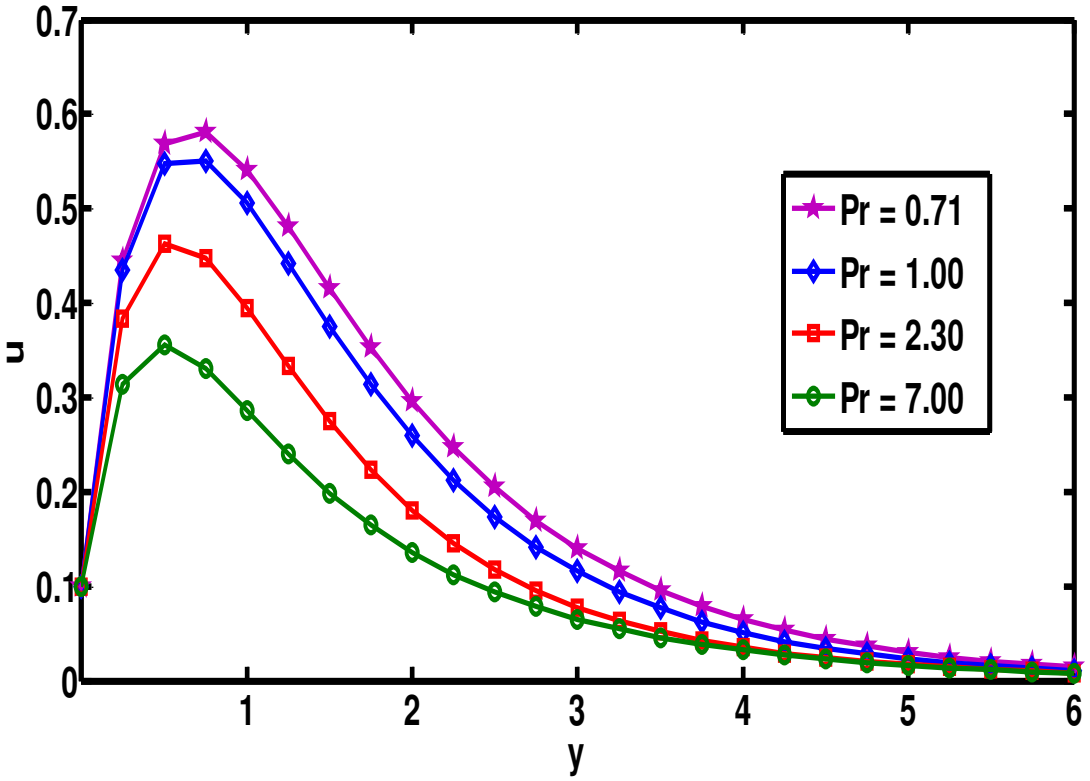

Figure 9: The u(y) profiles for Prandtl number Pr

International Journal For Recent Developments in Science & Technology
2581-4575
Crossref
A Peer Reviewed Research Journal

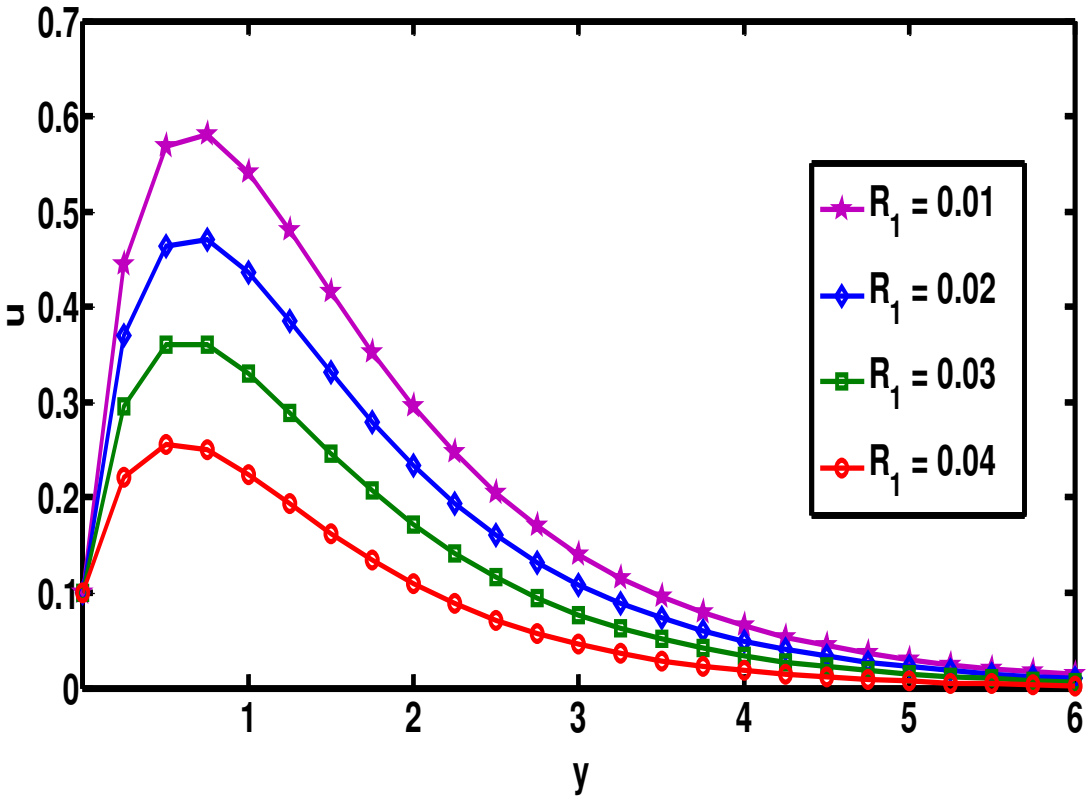

Figure 10: The u(y) profiles for Radiation Absorption Parameter R_1

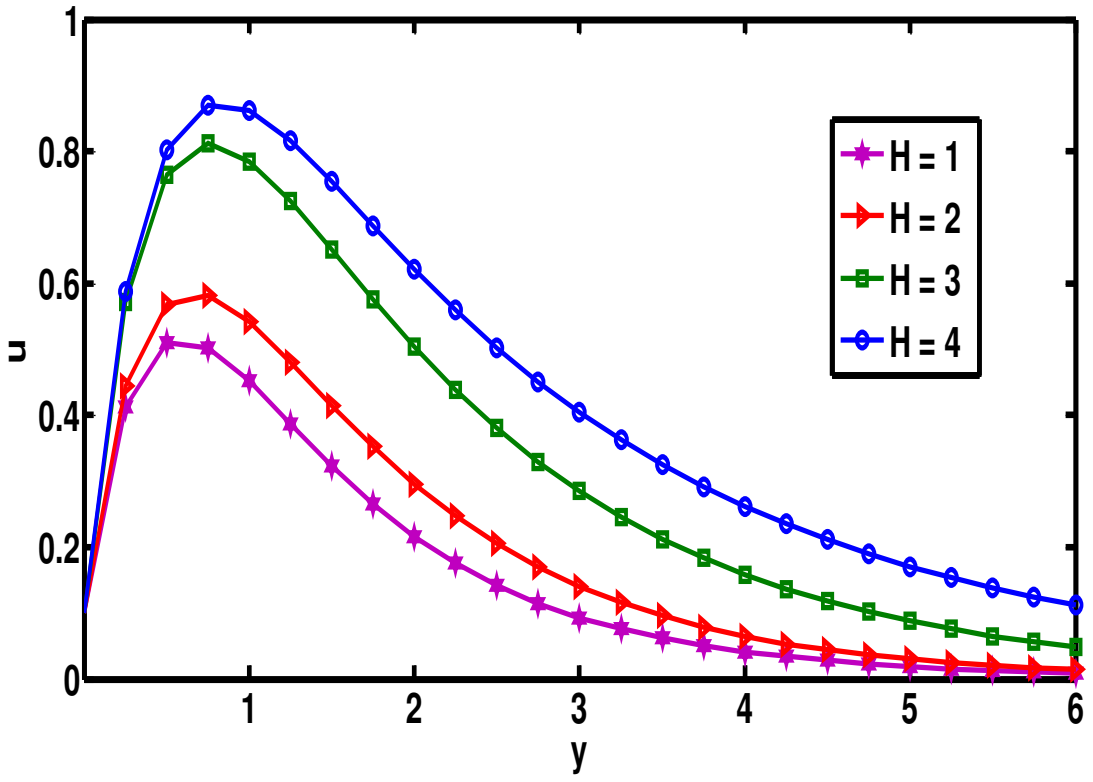

Figure 11: The u(y) profiles for heat source parameter H.

International Journal For Recent Developments in Science & Technology
2581-4575
Crossref
A Peer Reviewed Research Journal

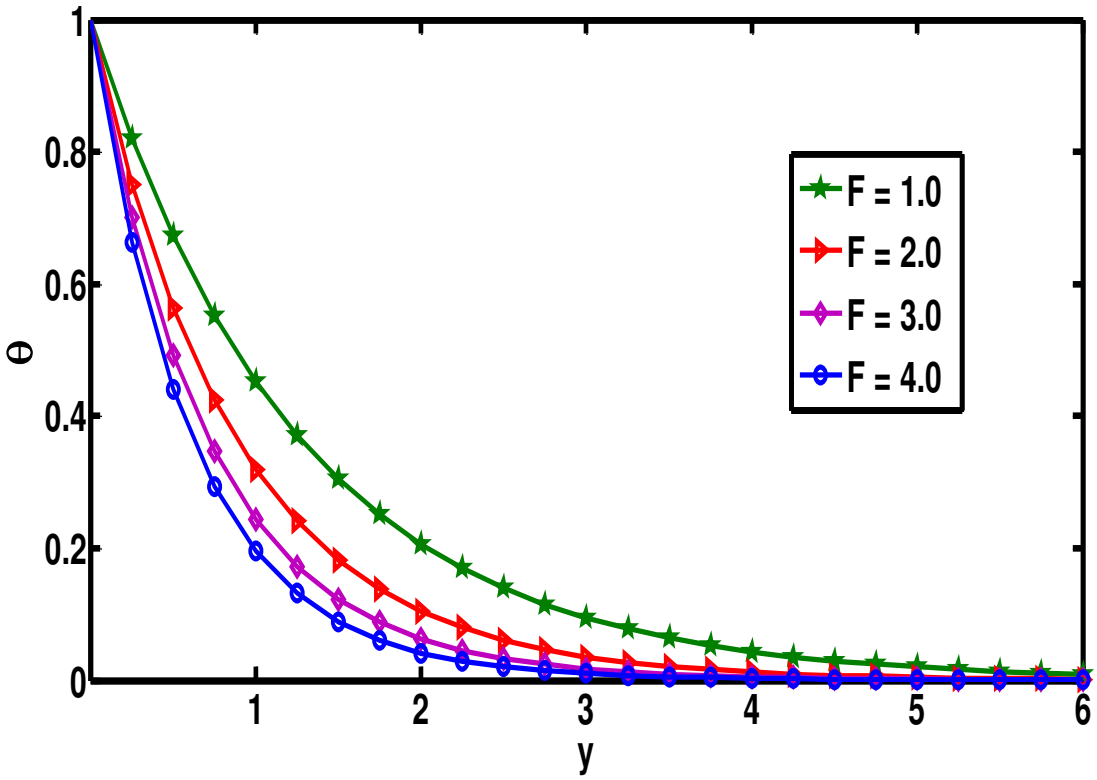

Figure 12: The θ(y) profiles for radiation parameter F

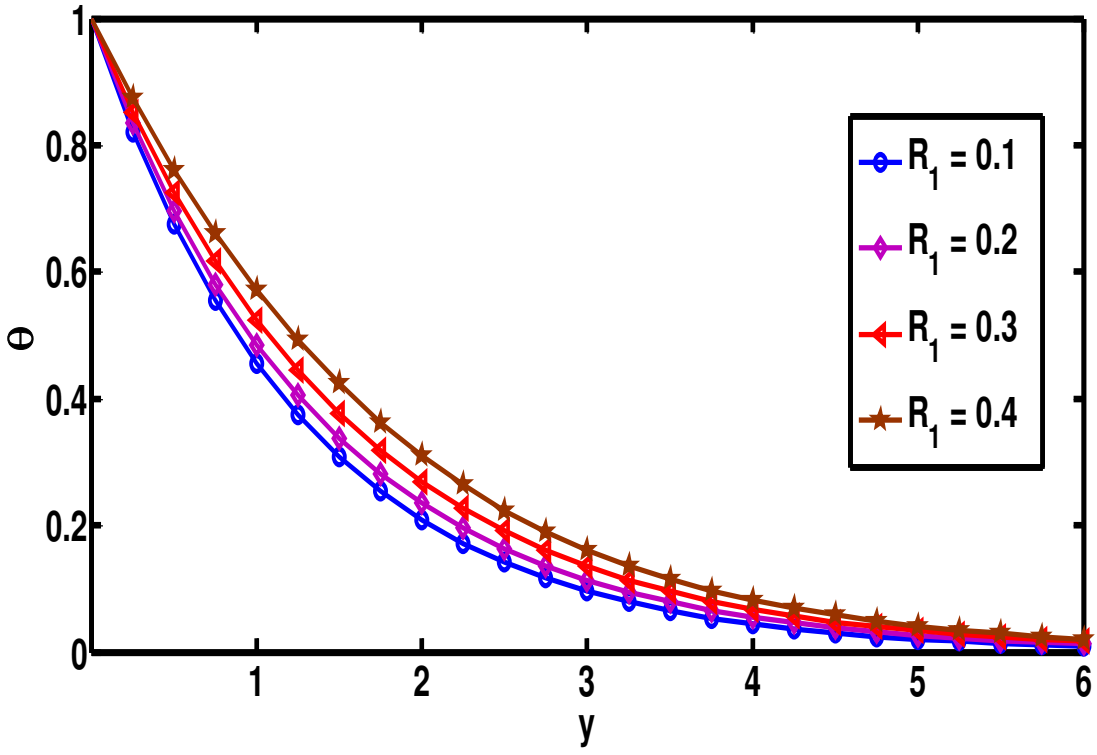

International Journal For Recent Developments in Science & Technology
2581-4575
Crossref
A Peer Reviewed Research Journal

Figure 13: The θ(y) profiles for R_1.

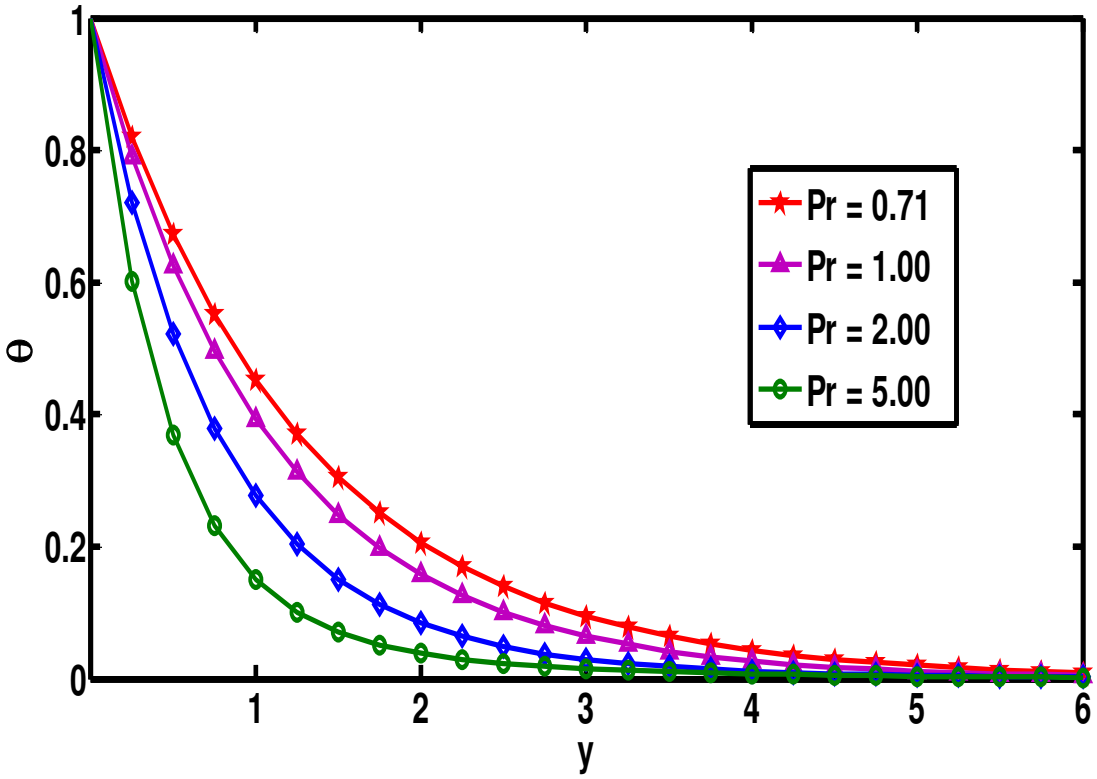

Figure 14: The θ(y) profiles for Prandtl number Pr

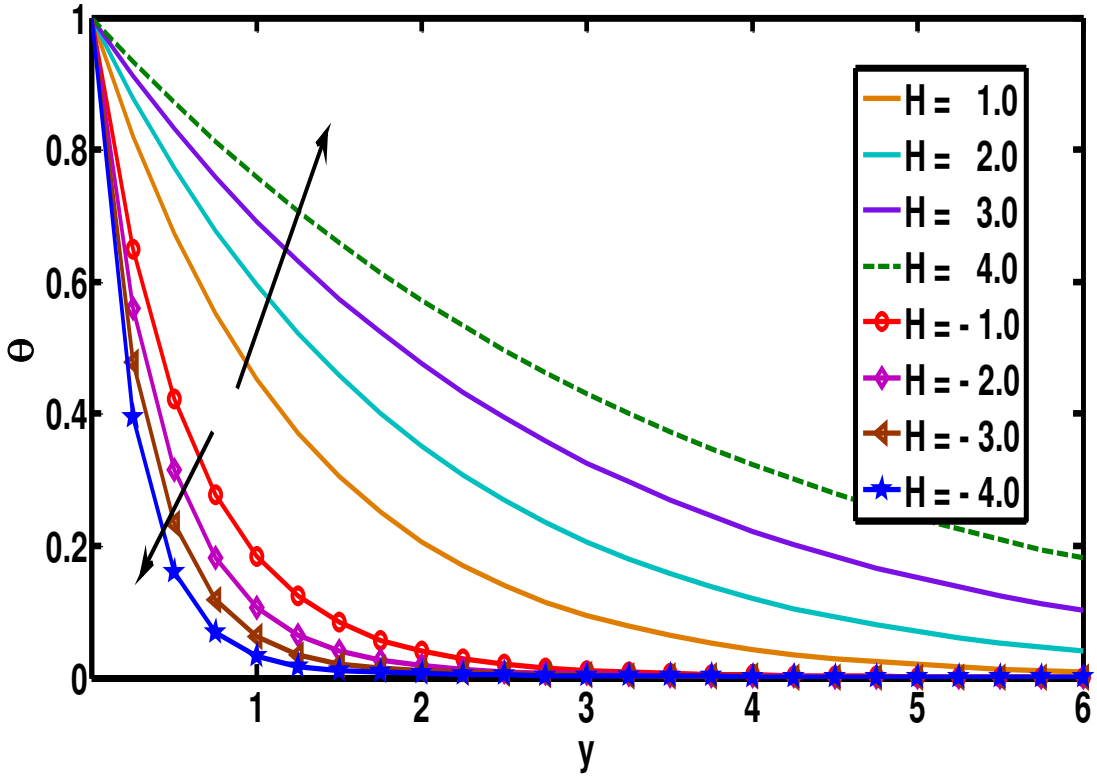

International Journal For Recent Developments in Science & Technology
2581-4575
Crossref
A Peer Reviewed Research Journal

Figure 15: The θ(y) profiles for Heat source parameter H

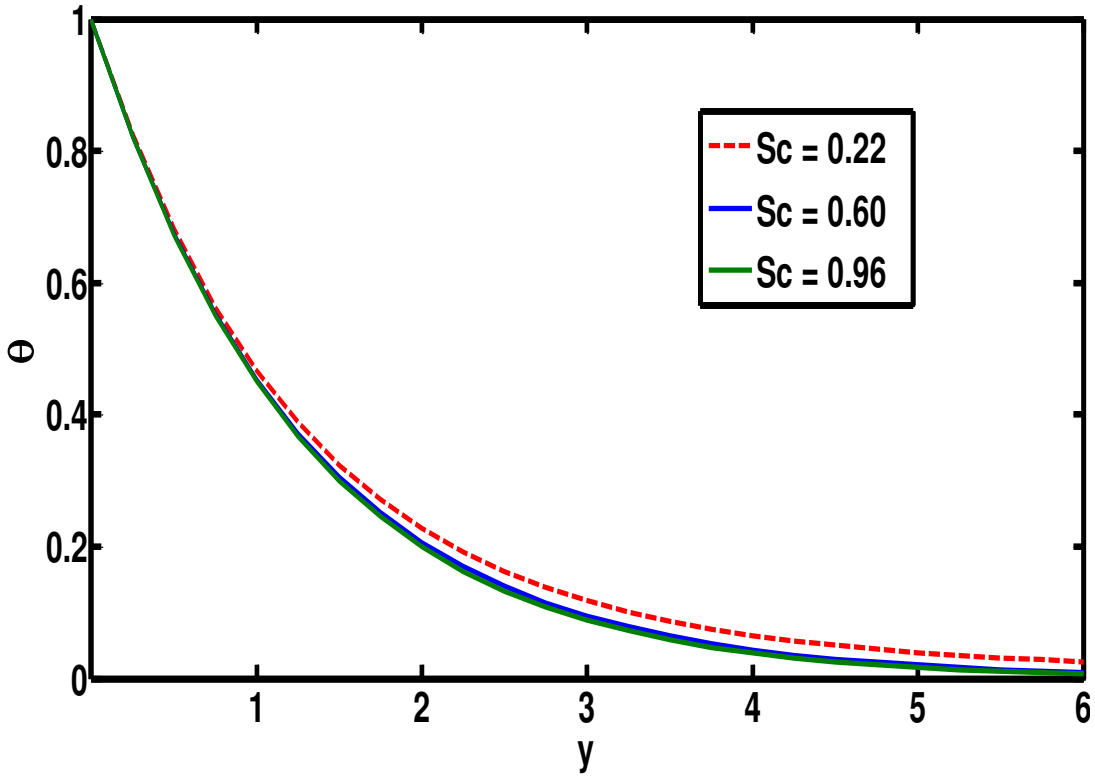

Figure 16: The θ(y) profiles for Schmidt number Sc.

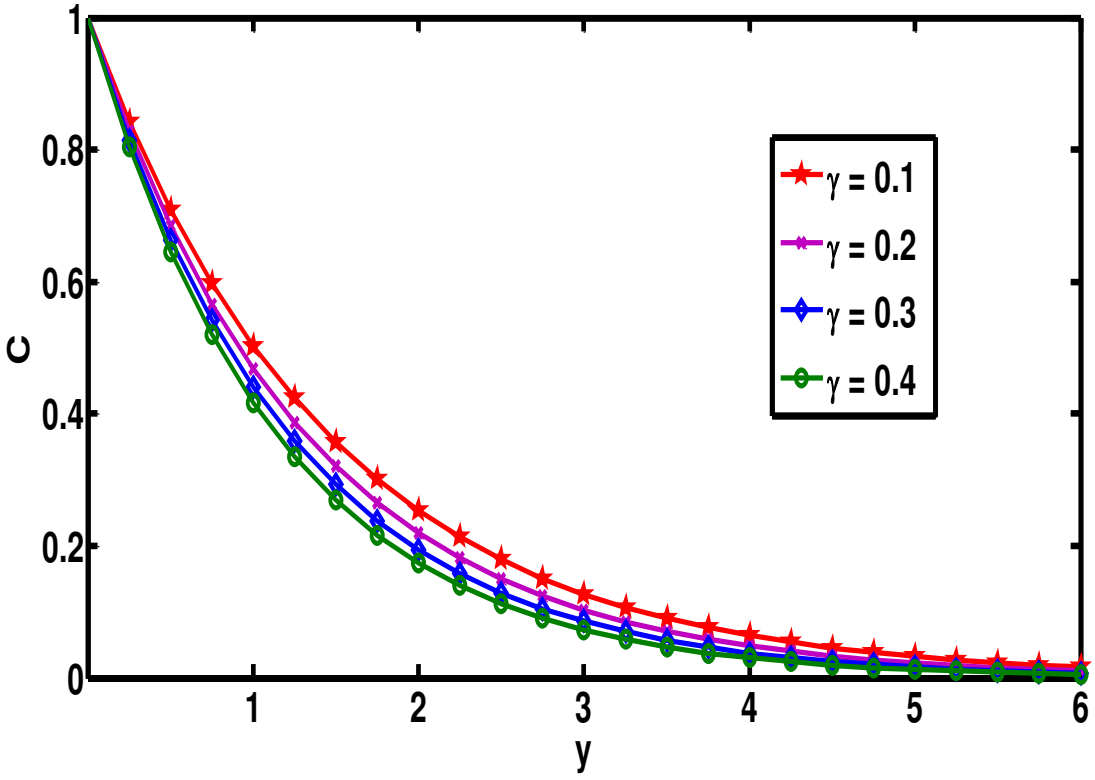

International Journal For Recent Developments in Science & Technology
2581-4575
Crossref
A Peer Reviewed Research Journal

Figure 17: The C(y) profiles for Chemical reaction parameter γ

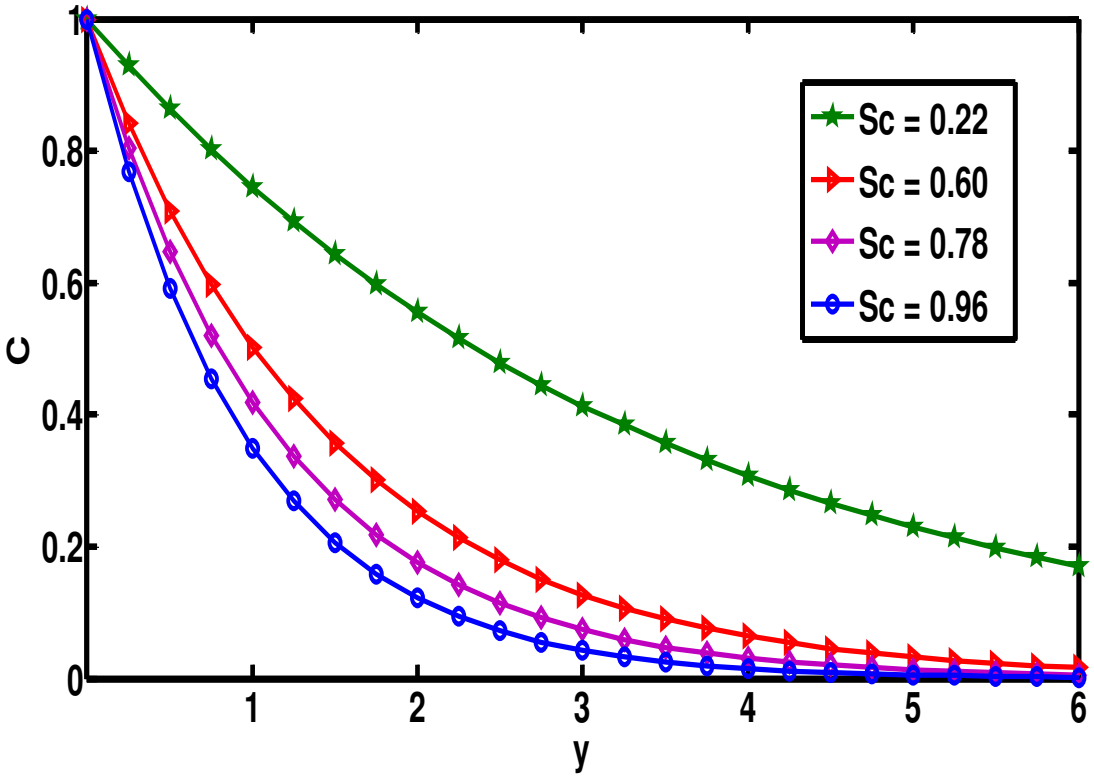

Figure 18: The C(y) profiles for Schmidt number Sc.

5. CONCLUSIONS:

The impact of radiation absorption, viscosity, and joules dissipation on chemically reactive and radiative flow in MHD free convection on a moving inclined porous plate with a temperature dependent heat source is investigated via a theoretical analysis. The perturbation method yields exact solutions to equations. The study's findings are as follows:

- Velocity upsurges with the growth of K and F and reductions with the intensification of M and α.
- Upsurge of Gr, R_1, Pr and Sc leads to lessening of velocity.
- Temperature diminutions with the rise of F, Pr and Sc and growths with the rise of R_1.
- Concentration shrinkages as Sc and γ upsurges.

References:

1) Huang X, Gollner MJ. Correlations for evaluation of fame spread over an inclined fuel surface. Fire Saf Sci. 2014;11:222–33.

2) Cheng P. Film condensation along an inclined surface in a porous medium. Int J Heat Mass Transf. 1981;24:983–90.

3) Bég OA, Zueco J, Chang TB. Numerical analysis of hydromagnetic gravity-driven thin film micropolar fow along an inclined plane. Chem Eng Comm. 2010;198(3):312–31.

4) Balmforth NJ, et al. Viscoplastic flow over an inclined surface. J Non-Newton Fluid Mech. 2007;142(1–3):219–43.
5) Ashraf MB, et al. Radiative mixed convection flow of an Oldroyd-B fluid over an inclined stretching surface. J Appl Mech Tech Phys. 2016;57:317–25.
6) Pruess K, Zhang Y. A hybrid semi-analytical and numerical method for modeling wellbore heat transmission. In: Proceedings of 30th workshop on geothermal reservoir engineering, Stanford University, Stanford, California, USA (2005).
7) Greener Y, Middleman S. Blade-coating of a viscoelastic fluid. Poly Eng Sci. 1974;14:791–6.
8) Chang H-C, Demekhin EA. Complex wave dynamics on thin films. Amsterdam: Elsevier; 2002.
9) Ilias MR, Rawi NA. Steady aligned MHD free convection of ferro fluids flow over an inclined plate. J Mech Eng. 2017;4(2):1–15.
10) Johnson AF. Rheology of thermoplastic composites I. Compos Manuf. 1995;6:153–60.
11) Nsom B, Ramifdisoa L, Latrache N, Ghaemizadeh F. Linear stability of shear-thinning fluid down an inclined plane. J Mol Liq. 2019;227:1036–46.
12) Mukhopadhyay A, Chattopadhyay S. Long wave instability of thin film flowing down an inclined plane with linear variation of thermophysical properties for very small Biot number. Int J NonLinear Mech. 2018;100:20–9.
13) Mehmood OU, Maskeen MM, Zeeshan A. Hydromagnetic transport of dust particles in gas fow over an inclined plane with thermal radiation. Res Phys. 2017;7:1932–9.
14) Roy NepalC, Hossain Anwar, Gorla RSR. Combustible boundarylayer fows along inclined hot surfaces with streamwise surface temperature variations. J Thermophys Heat Trans. 2018. https:// doi.org/10.2514/1.T5465.
15) Sulochana C, Ashwinkumar GP, Sandeep N. Effect of frictional heating on mixed convection flow of chemically reacting radiative Casson nanofuid over an inclined porous plate. Alex Eng J. 2017. https://doi.org/10.1016/j.aej.2017.08.006.
16) Sui Jize, Zheng Liancun, Zhang Xinxin, Chen Goong. Mixed convection heat transfer in power law fuids over a moving conveyor along an inclined plate. Int J Heat Mass Trans. 2015;85:1023–33.
17) Guha Abhijit, Jain Akshat, Pradhan Kaustav. Computation and physical explanation of the thermos-fluid-dynamics of natural convection around heated inclined plates with inclination varying from horizontal to vertical. Int J Heat Mass Tranf. 2019;135:1130–51.
18) RamReddy P, Naveen P, Srinivasacharya D. Influence of nonlinear Boussinesq approximation on natural convective fow of a power-law fluid along an inclined plate under convective thermal boundary condition. Nonlinear Eng. 2018. https://doi.org/10.1515/ nleng-2017-0138.
19) RamReddy Ch, Naveen P, Srinivasacharya D. Nonlinear convective flow of non-Newtonian fluid over an inclined plate with convective surface condition: a Darcy-

International Journal For Recent Developments in Science & Technology
2581-4575
Crossref
A Peer Reviewed Research Journal


Forchheimer Model. Int J Appl Comput Math. 2018. https://doi.org/10.1007/s40819-018-0484-z.

20) RamReddy Ch, Naveen P, Srinivasacharya D. Quadratic convective flow of a micropolar fuid along an inclined plate in a non-Darcy porous medium with convective boundary condition. Nonlinear Eng. 2017. https://doi.org/10.1515/nleng-2016-0073.